Available online at www.worldscientificnews.com

World Scientific News

WSN 60 (2016) 92-102 EISSN 2392-2192

The Magnetic Moments of Single-Domain and its Mathematics Formation

Sabah Jameel Mezher

Department of Physics, College of Science, AL-Mustansirya University, Bahgdad, Iraq

E-mail address: Sabah_su2010@yahoo.com

ABSTRACT

We now demonstrate that such "uniaxial" particles can allow several quantifiable stable (or metastable) orientations of the magnetic moment within the same particle. A new model is presented with quantitative predictions verified by experiments. The results have important implications for rock magnetism, palaeomagnetism, and magnetic materials research. Firstly, the new model quantitatively accounts for several previously unexplained diverse phenomena exhibited by such single-domain (SD) particles. Including the acquisition of gyroremanences, tiled-impressed anisotropy, and transverse components of reminisce in individual particles. These phenomena are theoretically impossible in idealized uniaxial single domain particles, and could now be used to quantify the deviation of real particles from ideal behavior. Secondly, deflections of the natural remanence vector and computations of the ancient field vector and paleointensity are not only controlled by the shape and distribution of the particles, but also by the possible stable orientations of the moments within single-domain particles. The model is also relevant to other single-domain particle morphologies.

***Keywords*:** Magnetic Moments; Single domain; uniaxial particles; rock magnetism; palaeomagnetism; magnetic materials; diverse phenomena

1. INTRODUCTION

The domain theory explains magnetic phenomenon by proposing the existence of domains. Domains are small regions within an object that are magnetic. These regions may be from one to hundreds of microns, which is small, but larger than atomic in size.

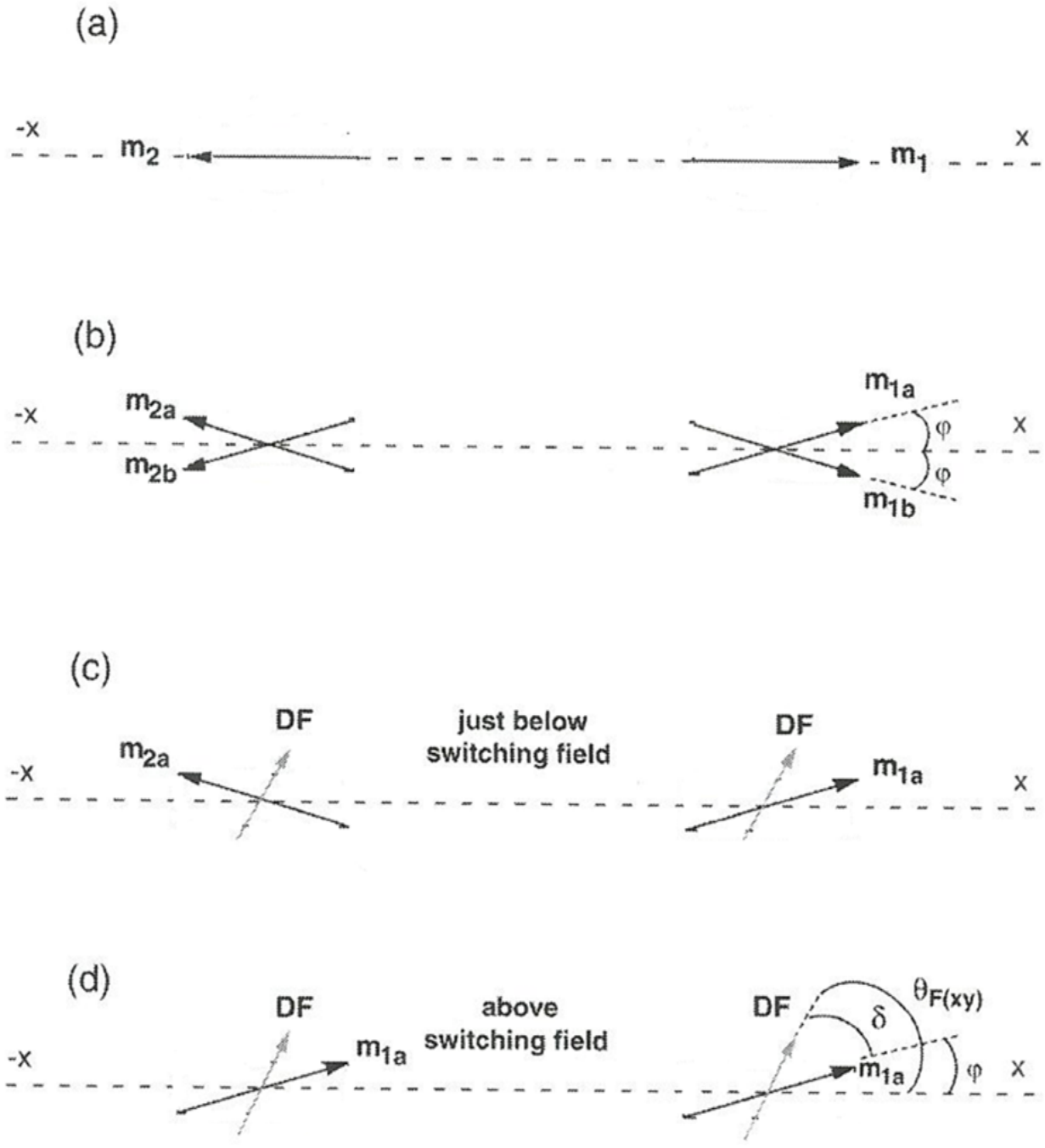

Figure 1. (a) Schematic of idealized uniaxial SD particles (prolate ellipsoids). The moment has only two possible opposing stable moment orientations (m_1 and m_2). **(b)** Schematic of real "uniaxial" acicular SD particles showing the range of possible "parallel" and "anti- parallel" moment positions (m_{1a} to m_{1b}, and m_{2a} tom$_{2b}$) as proposed in the new model. **(c)** A steep DF (direct field) below the switching field orients the respective moments towards m_{1a} and m_{2a} , where they can remain after the field is removed. **(d)** Above the switching field the DF orients all the moments towards m_{1a}.

When the polarities of the individual domains are randomized, their fields cancel one another and the object is not magnetic. When the polarities of all domains are parallel and aligned, their fields reinforce one another and the object is magnetic. This theory explains several observations. When a ferrous material such as a nail is left in a magnetic field for an extended period of time the material becomes magnetic, at least temporarily.

The explanation is that the domains are subject to atomic jostling and move randomly about fixed points. When exposed for a time to a magnetic field, the domains eventually line up with the field much as a compass needle lines up with the Earth's magnetic field. Once the domains are aligned, the object as a whole acts as a magnet. When removed from the field the jostling eventually randomizes the field again and the material becomes demagnetized. Magnets become demagnetized when heated or when hammered or dropped repeatedly. This treatment randomizes the orientation of the domains which causes their individual fields to cancel.

An idealized uniaxial stable single-domain (SD) particle has only two possible stable states (Figure 1(a)) in which the moment can lie [l]. In nominal "uniaxial" SD particles, such as acicular γ-Fe_2O_3 particles, this implicit two state feature has never been challenged, whilst there has been considerable debate concerning the mechanism of moment reversal between the two states. However, any model of such particles has to explain several observed phenomena, which theoretically should not occur in idealized uniaxial SD particles. These include transverse components of remanence in individual particles [2], field- impressed anisotropy [3-5], and gyroremanences [6-9]. The present paper will demonstrate that a new simple model of "uniaxial" SD magnetic moments can quantitatively explain these diverse phenomena. New predictions are verified by further experiments. The implications of the new model for improving computations of the ancient field vector and palaeointensity in anisotropic rocks will also be briefly discussed.

2. MATHEMATICAL EXPLANATION

We can get an accurate relationship for the distribution of magnetization in the limit of 180º within the domain when there is no applied magnetics external field $\left(\vec{H}_{app} = 0\right)$, the ferromagnetic energy density get by the relation [10]:

$$W = \left[\tilde{A}\left(\frac{\partial \vec{M}_s}{\partial x}\right)^2 - \tilde{K}_u\left(\vec{M}_{sz}\right)^2 - \frac{1}{8\pi}\vec{H}_{dem}^2\right] \dots\dots\dots\dots\dots (1)$$

$\vec{H}_{dem}$is the Demagnetizing field which equal to:

$$\vec{H}_{dem} = -N_d\vec{M}_s = -N_d\begin{bmatrix}\vec{M}_{sx}\\ \vec{M}_{sy}\\ \vec{M}_{sz}\end{bmatrix} = \begin{bmatrix}\vec{H}_{dem_x}\\ \vec{H}_{dem_y}\\ \vec{H}_{dem_z}\end{bmatrix} \dots\dots\dots (2)$$

where N_d is Demagnetizing Factor. We can write the magnetization vector as:

$$\vec{M}_s = \begin{pmatrix} \vec{M}_{sx} \\ \vec{M}_{sy} \\ \vec{M}_{sz} \end{pmatrix} = M_s \begin{pmatrix} sin\theta \sin\varphi \\ \sin\theta \cos\varphi \\ \cos\theta \end{pmatrix} \ldots\ldots\ldots\ldots\ldots (3)$$

The amount of magnetizing can be fixed $(i.e\ |M_s| = const.)$, so the system state is completely described by θ(x) and φ(x). If compensation equations (2) and (3) in the equation (1), we get the following:

$$W = A\left[\left(\frac{\partial\theta}{\partial x}\right)^2 + \left(\frac{\partial\varphi}{\partial x}\right)^2 sin^2\theta\right] - K_u\, cos^2\theta + \frac{(N_d)^2}{8\pi} M_s{}^2 sin^2\,\varphi\, sin^2\,\theta \quad \ldots (4)$$

and by put the following boundary conditions:

$$\begin{aligned} &\theta(-\infty) = 0 \\ &\theta\,(-\infty) = \pi \quad \ldots\ldots\ldots\ldots\ldots\ldots\ldots\ldots (5) \\ &\varphi\,(x) = cost. \end{aligned}$$

Then use the calculus of variations:

$$\delta\, W = 2A\theta'\,\delta\,\theta' + 2\left[K_u + \frac{(N_d)^2}{8\pi} M_s{}^2 sin^2\,\varphi\right] \sin\theta\cos\theta\delta\theta \qquad \ldots\ldots\ldots (6)$$

when ($\theta' = \frac{d\theta}{dx}$) and

$$\delta_{\varepsilon_{mag}}(\vec{M}_s) = \int_{-\infty}^{\infty} \delta W dV$$

In which (dV) represents a volume component, than:

$$\delta\varepsilon_{mag} = \int_{-\infty}^{\infty}\left[2A\theta'\delta\theta' + 2\left[K_u + \frac{(N_d)^2}{8\pi} M_s^2 sin^2\varphi\right] sin\theta cos\theta\delta\theta\right] dx \quad \ldots\ldots (7)$$

$$\delta_{\varepsilon_{mag}} = \int_{-\infty}^{\infty} 2A\theta'\delta\,\theta' dx + \int_{-\infty}^{\infty} 2\left[K_u + \frac{(N_d)^2}{8\pi} M_s^2 sin^2\varphi\right] \sin\theta\cos\theta\delta\theta\, dx \quad \ldots (8)$$

and the integration of the first part gets:

$$\int_{-\infty}^{\infty} 2A\theta'\delta\theta' dx = [2A\theta'\delta\theta']_{-\infty}^{\infty} - \int_{-\infty}^{\infty} 2A\theta''\delta\theta\, dx \qquad \ldots\ldots\ldots (9)$$

$$\therefore\ \delta_{\varepsilon_{mag}}\left(\vec{M}_s\right) = \int_{-\infty}^{\infty}\left[-2A\theta''\delta\theta + 2\left[K_u + \frac{(N_d)^2}{8\pi}M_s^2 sin^2\theta\right]sin\theta cos\theta\delta\theta\right]dx \quad \ldots\ldots\ldots\ldots(10)$$

$$\therefore\ \delta W = -2A\theta''\delta\theta + 2\left[K_u + \frac{(N_d)^2}{8\pi}M_s^2 sin^2\varphi\right]sin\theta cos\theta\delta\theta \quad \ldots\ldots\ldots\ldots(11)$$

$$\frac{\delta w}{\delta\theta} = -2A\theta'' + 2\left[K_u + \frac{(N_d)^2}{8\pi}M_s^2 sin^2\varphi\right]sin\theta cos\theta \quad \ldots\ldots\ldots\ldots\ldots\ldots(12)$$

and by making the ferromagnetic energy density less $\left(i.e\ \frac{\delta W}{\delta\theta} = 0\right)$ then:

$$\therefore\ \left[\frac{A}{K_u + \frac{(N_d)^2}{8\pi}M_s^2 sin^2\varphi}\right]\theta'' - sin\theta cos\theta\delta\theta = 0 \quad \ldots\ldots\ldots\ldots\ldots\ldots(13)$$

$$\Delta_\circ(\varphi) = \sqrt{\frac{A}{K_u + \frac{(N_d)^2}{8\pi}M_s^2 sin^2\varphi}} \quad \ldots\ldots\ldots\ldots\ldots(14)$$

where $(\Delta_\circ)$ is a distinctive fish reducing magnetic domain resulting from the competitive effects of the various contributions for the effective field. Since the wall Bloch is described by the relation $[\varphi(x) = 0]$, then:

$$\Delta_\circ = \sqrt{\frac{A}{K_u}} \quad \ldots\ldots\ldots\ldots\ldots\ldots\ldots(15)$$

Since the change in the magnetization direction within the limit of the domain over 180º, the width border domain (Δ) is:

$$\Delta = \pi\sqrt{\frac{A}{K_u}} = \pi\,\Delta_\circ \quad \ldots\ldots\ldots\ldots\ldots\ldots(16)$$

The magnetization often imposes be replicated within smaller areas of about half a distinctive and Showing domain differs from the special offer border domain by factor (π).

When compensation$(\Delta_\circ)$ in the equation (13) we get the following:

$$\Delta_\circ^2\theta'' - sin\theta cos\theta\delta\theta = 0 \quad \ldots\ldots\ldots\ldots\ldots\ldots(17)$$

and by multiplying both sides of the equation (17) by $\frac{d\theta}{dx}$ and anintegration, we find that:

$$\Delta_{\circ}^{2}\frac{\theta'^{2}}{2}-\frac{sin^{2}\theta}{2}=c \qquad \ldots\ldots\ldots\ldots\ldots\ldots\ldots\ldots(18)$$

Now, by using the boundary conditions of the equation (5), we get that c = 0 and:

$$\therefore\ \Delta_{\circ}^{2}\frac{\theta'^{2}}{2}-\frac{sin^{2}\theta}{2}=0 \qquad \ldots\ldots\ldots\ldots\ldots\ldots\ldots(19)$$

$$\theta'=\frac{\sin\theta}{\Delta_{\circ}} \qquad \ldots\ldots\ldots\ldots\ldots\ldots\ldots\ldots(20)$$

$$\theta(x)=2\,tan^{-1}\left[exp\left(\pm\frac{x}{\Delta_{\circ}}\right)\right] \qquad \ldots\ldots\ldots\ldots\ldots\ldots\ldots\ldots(21)$$

where the above equation represents the distribution of magnetization in the border domain.

3. A NEW MODEL OF STABLE SD MOMENTS

A new model is proposed whereby the moment of an acicular (cylindrical) "uniaxial" SD particle has several stable (or metastable) positions. It is further proposed that the range of stable positions is influenced by the aspect ratio of the particle, being constrained within parallel and anti-parallel cones whose angular dimension $\varphi = \tan^{-1}$ [particle diameter / particle length]. Figure l (b) shows a side cross- sectional view (arbitrarily in the xy plane) of the range of parallel (m_{1a} to m_{1b}) and anti-parallel (m_{2a} to m_{2b}) stable moment positions. There may also be more extreme positions of the moment. Especially if strong fields are applied perpendicular to the particle long axis, and also in irregularly shaped particles (those that may not be perfect cylindrical shapes).

The model was quantitatively tested by examining the dependence of isothermal remnant magnetization, IRM, on applied field direction using a sample containing dilute dispersed (0.03% by volume) acicular SD y-Fe_20_3 particle (l μm in length and 0.22 μm in diameter). The particles were set in resin in the presence of a direct field(DF) of l00 mTalong the x-axis. This should ideally have aligned all the particle long axes along x (scanning electron microscopy images on one flat end face of the sample were consistent with this). If the sample comprised ideal uniaxial SD particles fully aligned in the x-axis, any subsequent imparted remanence would remain along x regardless of the applied field direction.

If the sample comprised ideal uniaxial SD particles partially aligned along x, then the resulting remanence vector due to any misaligned particles should be coincident with that theoretically calculated using the sample's IRM anisotropy ellipsoid [11]. lf the particles are aligned along x, but the moments have a range of possible stable positions within ± φ as proposed in the new model, then the sample's resultant remanence direction will be oriented up to ± φ degrees from the x- axis for applied fields above the switching field of the particles .

For a relatively steep orientation of the DF the model predicts that as the field strength is increased above the switching field the remanence direction will saturate at the orientation φ, since more and more moments switch from m_{2a}, (Figure l(c)) to m_{1a} (Figure l(d)).

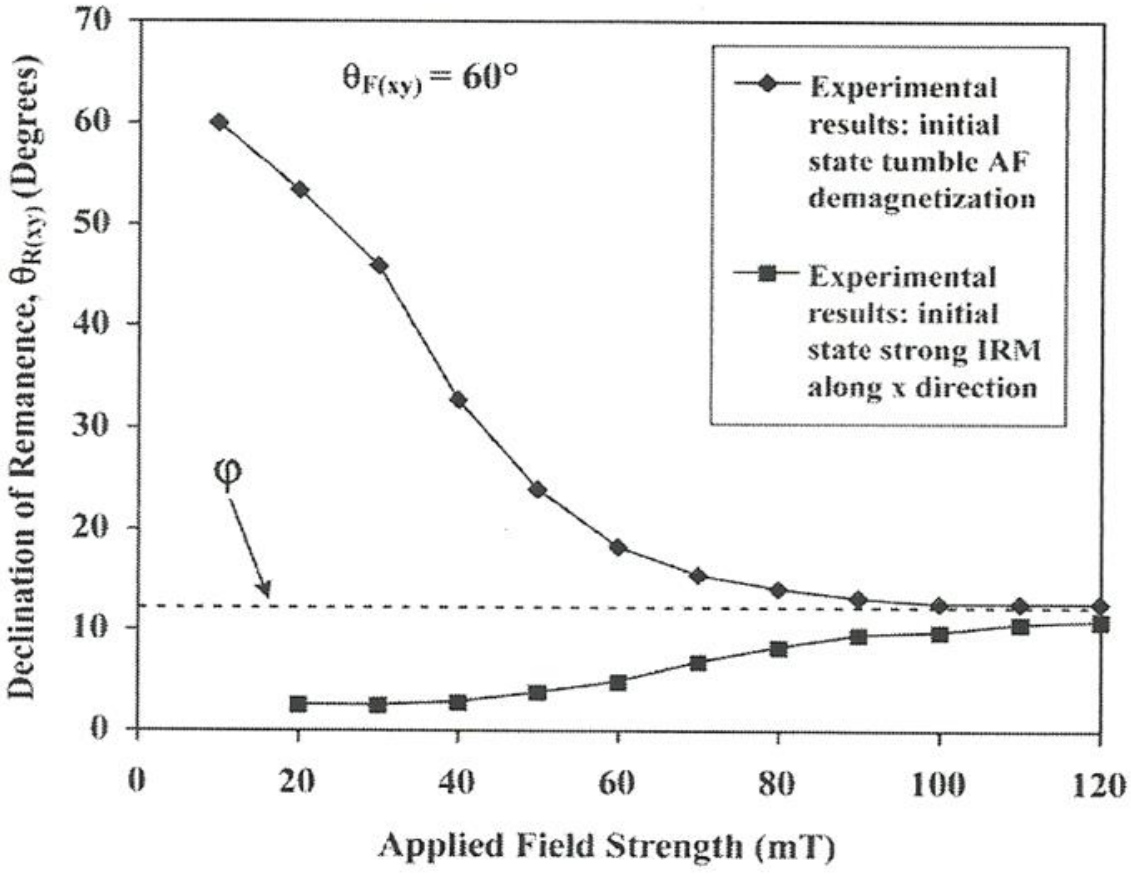

Figure 2. Applied field strength versus declination of remanence for a DF oriented in the xy plane at a declination $\theta_{F(xy)}$ = +60° (and inclination = 0°) for a dilute dispersion of SD γ-FeZO3 particles aligned along the x- axis. The ratio particle length / diameter = 4.5 (φ = 12.53º). Results for two different initial states are shown: after tumble AF demagnetization, and after a strong (100 mT) IRM was initially applied along the x direction.

Figure (2) demonstrates this for a relatively steep DF applied in the xy plane at a declination $\theta_{F(xy)}$ = +60°. As the applied DF is increased in strength from an initially tumble alternating field (AF) demagnetized state, the declination of remanence, $\theta_{R(xy)}$, saturates at almost exactly the theoretical value of φ (l2.53°) for these particles (aspect ratio 4.5). This is significantly different from the computed declination (28.3°) from the sample‘s IRM anisotropy ellipsoid (whose principal axes are oriented along the x, y and z sample axes). Moreover, $\theta_{R(xy)}$ also saturates at φ when the sample is initially given a strong DF along x (aligning the moments along X) and a DF then applied at increasing strengths at $\theta_{F(xy)}$ = +60º .

A range of other applied field orientations was tested. Figure (3) shows the experimental results (squares) for a 120 mT DF applied at various declinations, $\theta_{F(xy)}$, in the xy plane of the sample. Tumble AF demagnetization was employed prior to each DF application. The results are not consistent with ideal uniaxial SD particles fully aligned along x, except at very small angles of $\theta_{F(xy)}$. They are also significantly different to the computed

values (diamonds) using the sample's IRM anisotropy ellipsoid [11] at I20 mT, and are thus inconsistent with a distribution of partially aligned ideal SD uniaxial particles.

The new model, however, is consistent with the experimental results. For shallow and moderate applied field orientations the declination is no greater than φ. Significantly, there is a distinct plateau at φ at moderately steep angles, which is consistent with the model. At very steep values of $\theta_{F(xy)}$, for example the results at $\theta_{F(xy)} = +75°$, the 120 mT applied field may not be above the switching field [l2], which may explain why $\theta_{R(xy)} > \varphi$ for this orientation. (Note we believe particle interactions play a negligible role in our results, since the particles are dilute dispersed and the sample exhibits SD susceptibility versus remanence anisotropy characteristics typical of non-interacting particles. Also, results on isotropic dilute dispersions of SD maghemite and hematite, where the particles were not set in a magnetic field, are also consistent with the new model as detailed later).

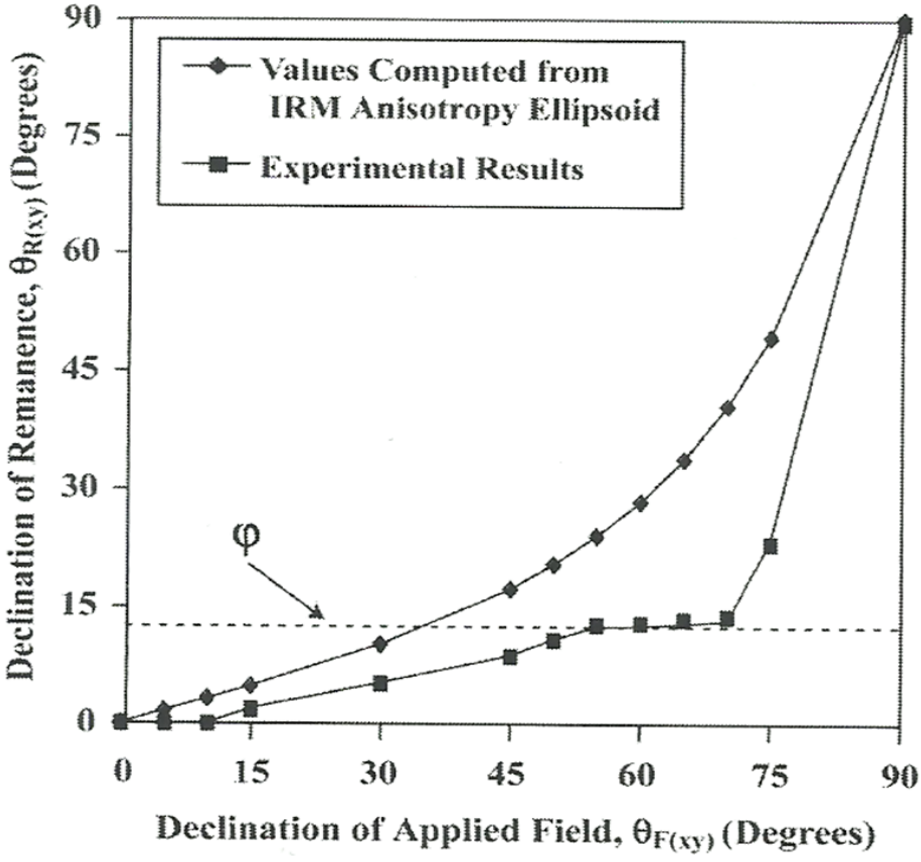

Figure 3. The relationship between the applied (120 mT) DF direction in the xy plane, $\theta_{F(xy)}$, and the remanence direction, $\theta_{R(xy)}$, for a dilute dispersion of SD γ-Fe_2O_3 particles (aspect ratio 4.5; φ = l2.53°) aligned along the x- axis. Errors are smaller than the symbol size. Squares are experimental results. Diamonds are computed values [11] using the field directions and the sample's IRM anisotropy ellipsoid at l20 mT. Ideal uniaxial SD particles fully aligned in the x-axis would have plotted solely along the x-axis.

4. EXPLANATION FOR FIELD-IMPRESSED ANISOTROPY EFFECTS IN SD PARTICLES

Theoretically, a strong AF or DF applied to an ideal uniaxial SD particle should not cause its low field susceptibility anisotropy to change, since the two possible states shown in Figure 1(a) are effectively identical as regards reversible susceptibility in a weak AF. By a similar argument a distribution of such particles should not exhibit any difference in susceptibility between the demagnetized and magnetized states. Therefore, observations of field-impressed susceptibility anisotropy in dilutely dispersed "uniaxial" SD particles from magnetic tape [3,4] and rocks [5] require an explanation.

However, if SD particles have a range of stable moment positions then these effects can be explained. For example, after tumble AF demagnetization the moment of an acicular SD particle could be orientated within the range of possible stable positions shown in Figure l(b). When a strong DF is subsequently applied parallel to the particle long X- axis the moment will re-align along this axis and remain there once the field is removed. This will change the particle's susceptibility, unless the moment was already in this orientation, resulting in a minimum susceptibility parallel to x. (Note that an ideal uniaxial SD particle has zero susceptibility parallel to its long axis [11]).

Table 1. Correlations between φ, field-impressed anisotropy (after a DF of 80 mT) and RRM (at 95 r.p.s., in an AF of 80 mT).

Particle Type	φ (Degrees)	Field-Impressed Anisotropy A_{fs} (%)	RRM (10^{-3} Am^2 kg^{-1})
Idealised Uniaxial SD	0	0	0
SD γ-Fe_2O_3 (Aspect ratio 6.5)	8.75	-1.22	226
SD γ-Fe_2O_3 (Aspect ratio 4.5)	12.53	-1.73	335
SD α-Fe_2O_3 (Equant platelets)	60.00	-8.93	N/A

Likewise for a random distribution of acicular SD particles, our model predicts that the applied field impresses a susceptibility anisotropy represented by an ellipsoid of revolution with the unique minimum axis in the field axis, which is consistent with observations [3-5]. We now further predict that particles with lower values of φ (higher aspect ratios) should exhibit weaker field-impressed anisotropy, since more needle - like particles should be closer to ideal uniaxial behavior.

We tested this in two samples containing randomly distributed (isotropic) and dilutely dispersed (0.03% by volume) particles of SD γ-Fe_2O_3, with each sample containing particles of a different aspect ratio. In one sample the particle aspect ratio was 6.5 (φ = 8.75º) and in the other it was 4.5 (φ = l2.53°).

The application of an 80 mT DF caused percentage field-impressed susceptibility anisotropies of - l.22% and - l.73% respectively, where the negative sign indicates a decrease in susceptibility in the field direction and field- impressed anisotropy is defined by equation 7 of [4]. The impressed anisotropy values were directly proportional to so (inversely proportional to particle aspect ratio) confirming our predictions (Table 1). The model was also extended to SD hematite (α-Fe2O3). Here, at room temperature, the moment can lie in one of 3 possible easy axes, each separated by 60°, in the hexagonal basal plane.

With these three easy axes, then effectively φ = 60° with three possible "parallel" and three "anti-parallel" stable moment positions. We would therefore predict that SD hematite should exhibit a relatively high field- impressed anisotropy. The application of a DF of 80 mT to randomly and dilutely dispersed SD hematite particles in specular form did indeed result in a high percentage impressed susceptibility anisotropy of -8.93 %. Significantly, the result was in virtually the same direct proportion to go as for the SD γ-Fe2O3 samples (table I).

5. CONCLUSIONS

A new model relates the range of possible stable magnetic moment positions in a SD particle to quantifiable predictions of measureable bulk properties (susceptibility and remanence) in large distributions of such particles. The model provides quantitative explanations for field impressed effects, gyroremanences, and transverse components of remanence in acicular SD particles, all of which are theoretically impossible in ideal uniaxial SD particles. The deviation from ideal behavior can be quantified using these effects. New idealized particles (for media storage etc) could be designed and tested using these effects. Also, quantifying the range of stable moment positions within SD particles due to remanence acquisition will improve computations of the ancient field direction and palaeointensity from the NRM recorded in anisotropic rocks.

References

[1] Stoner E. C. and Wohlfarth E. P. 1948. A mechanism of magnetic hysteresis in heterogeneous alloys. *Phil. Trans. Roy. Soc.* A240, 599-642

[2] Knowles J. E. 1984. The measurement of the anisotropy field of single "tape" particles *IEEE Trans. Magnetics*, 20, 85-87

[3] Potter D. K. and Stephenson A. 1988. Field-induced magnetic anisotropy in a dilute dispersion of gamma - Fe_2O_3 particles. *J. App. Phys.* 63, 1691-1693.

[4] Potter D. K. and Stephenson A. 1990 a. Field-impressed anisotropies of magnetic susceptibility and remanence in minerals. *J. Geophys. Res. – Solia / Earth* 95, 15573-15588.

[5] Potter D. K. and Stephenson A. 1990 b. Field-impressed magnetic anisotropy in rocks. *Geophys. Res. Lett.* 17, 2437-2440.

[6] Stephenson A. 1980 a. Gyromagnetism and the remanence acquired by a rotating rock in an alternating magnetic field. *Nature* 284, 48-49.

[7] Stephenson A. 1980 b. A gyroremanent magnetization in anisotropic magnetic material. *Nature* 284, 49-51.

[8] Stephenson A. 1981. Gyromagnetic remanence and anisotropy in single-domain particles, rocks, and magnetic recording tape. *Phil. Mag.* B 44, 635-664.

[9] Stephenson A. and Potter D. K. 1987. Gyroremanent magnetizations in dilute anisotropic dispersions of gamma-ferric oxide particles from magnetic recording tape. *IEEE Trans. Magnetics*, 23, 3820-3830

[10] Faten Sajet, Study magnetic domains walls motion for ferromagnetic materials by using genetic algorithms. PhD thesis, AL-Mustansiryah University, College of Science, 2005.

[11] Stephenson A. Sadikun S. and Potter D. K. 1986. A theoretical and experimental comparison of the anisotropies of magnetic susceptibility and remanence in rocks and minerals. *Geophys. J. R. axlr. Soc.* 84, 185-200.

[12] Knowles J. E. 1988. A reply to “perfect and imperfect particles”. *IEEE Trans. Magnetics*, 24, 2263-2265.

(Received 10 November 2016; accepted 22 November 2016)